

FURTHER EXPLORATORY INVESTIGATIONS OF SOME SIMPLE CANDIDATE MANAGEMENT PROCEDURES FOR SOUTHERN BLUEFIN TUNA

D.S Butterworth, M. Miyagawa and M.R.A Jacobs¹

SUMMARY

Target-type CMPs for SBT presented to the Seattle meeting are refined and extended to include the input of CKMR information through use of the associated TRO index developed by Hillary. Essentially CMPs, tuned to median recovery to 30% of the pristine TRO in 2035, are developed for each of the CPUE, gene tagging and CKMR data sets alone, and then weighted combinations of these are considered. A subset of the robustness tests which show the greatest differences in performance compared to the base/reference case (RC) OM are selected. Overall the CMP based on the CKMR data only seems to perform best for the RC, but when the selected robustness test results are also taken into account, a variant based on a weighted combination of CMPs using all three data types seems marginally preferable.

要旨

この文章では、シアトル会議で発表したターゲット型のミナミマグロ管理方式をさらに改良・拡張し、Hillary氏が開発した総再生産出力 (TRO) 指標値を用いて、近縁遺伝標識再捕親子 (CKMR) 情報も管理方式に取り込んだ。CPUE、遺伝標識 (GT)、CKMR 情報それぞれを単独で考慮した資源管理方式に加え、それぞれの情報を重みづけして統合した管理方式も開発し、資源水準目標 (2035 年の TRO が初期のその 30%まで回復する) に 50%の確率で到達するようチューニングを行った。さらに、リファレンスセットと比べて最も影響が大きいと示唆されるいくつかの頑健性試験を選び出した。その結果、リファレンスセットに対しては、CKMR 情報のみを考慮した資源管理方式が最もパフォーマンスが優れていたが、頑健性試験も考慮すると、CPUE,GT,CKMR 全てのデータを統合して重みづけした管理方式のほうが若干パフォーマンスが優れていた。

Introduction

This paper extends analyses of CMPs for SBT first presented in Butterworth *et al.* (2018). Those analyses considered the application of simple target-type CMPs, first based on CPUE data only (DMM2), and then including gene tagging data as well (DMM3).

Here first the control parameters of the CMP using both CPUE and gene tagging data are adjusted to give improved performance (DMM4). Then a similar CMP based on CKMR data only (as summarized by the Hillary algorithm) is developed (DMM5), and finally a weighted combination of the earlier CMPs using all three types of data is put forward (DMM6).

¹ Marine Resource Assessment and Management Group (MARAM), Department of Mathematics and Applied Mathematics, University of Cape Town, Rondebosch 7701, South Africa

The robustness tests making the most impact on performance relative to that for the Base/Reference Case (RC) OM are then identified, and the performances of DMM4, DMM5 and DMM6 are compared for those tests.

Methods

First we define some aggregate indices, and follow this with the CMP specifications.

CPUE index

J_y is a relative CPUE index averaged over 5 years as follows:

$$J_y = \frac{(CPUE_{y-2} + CPUE_{y-3} + CPUE_{y-4} + CPUE_{y-5} + CPUE_{y-6}) \cdot \frac{1}{5}}{(CPUE_{2016} + CPUE_{2015} + CPUE_{2014} + CPUE_{2013} + CPUE_{2012}) \cdot \frac{1}{5}}$$

Sensitivities to this average over 3 years and 7 years have also been explored previously, and led to little difference in performance.

GT index

GTJ_y is a relative GT index averaged over 5 years as follows:

$$GTJ_y = \frac{(GTJ_{y-2} + GTJ_{y-3} + GTJ_{y-4} + GTJ_{y-5} + GTJ_{y-6}) \cdot \frac{1}{5}}{GTJ_{2016}}$$

CKMR index

$CKMR_y$ is a relative CKMR index averaged over 2 years as follows:

$$CKMR_y = \frac{(S_{y-5} + S_{y-6}) \cdot \frac{1}{2}}{(S_{2013} + S_{2012}) \cdot \frac{1}{2}}$$

where S_y is the estimated TRO value obtained from analyzing the CKMR-related data using the code kindly provided by Richard Hillary. Note that unlike the “directly observed” indices above (such as GTJ_{2016}), which remain fixed over time, here S_{2012} and S_{2013} will depend (slightly) on the year y for which $CKMR_y$ is being evaluated.

CMP specifications

DMM2

DMM2 was a CMP presented to the Seattle OMMP meeting using CPUE data only and based on the following formula, where β and J_{targ} are tuning parameters:

$$TAC_{y+1} = TAC_y \times (1 + \beta \cdot (J_y - J_{targ}))$$

DMM3

DMM3 extended DMM2 to also include gene tagging data, where now β , J_{targ} , γ and GTJ_{targ} are tuning parameters:

$$TAC_{y+1} = TAC_y \times (1 + \beta \cdot (J_y - J_{targ}) + \gamma(GTJ_y - GTJ_{targ}))$$

DMM4

At the time of the Seattle OMMP meeting, control parameter value choices and formula for DMM3 had yet to be finalized. The fourth CMP (DMM4) has completed this exercise by modifying the TAC formula in a way that better facilitates tuning, leading to the following formula and choices for the control parameter values.

$$\begin{aligned}TAC_{y+1}^1 &= TAC_y^1 \times (1 + \beta \cdot (J_y - J_{target})) \\TAC_{y+1}^2 &= TAC_y^2 \times (1 + \gamma \cdot (GTJ_y - GTJ_{target})) \\TAC_{y+1} &= w \cdot TAC_{y+1}^1 + (1 - w) \cdot TAC_{y+1}^2\end{aligned}$$

$$\beta = 0.05, J_{target} = 0.7, \gamma = 0.11, GTJ_{target} = 0.3, w = 0.7 .$$

Note that the γ and GTJ_{target} values were chosen first on the basis that the overall TRO tuning target for 2035 would be met if $w=0$ (i.e. the gene tagging data only were being used), and then selecting the combination that gave the narrowest PI for AAV during the projection period.

DMM5

The fifth CMP (DMM5) considers only the combined CKMR index generated from the TRO estimation method developed by Hillary *et al.* (2018).

$$TAC_{y+1} = TAC_y \times (1 + \kappa \cdot (CKMR_y - CKMR_{target}))$$

where $CKMR_{target}$ and the control parameter settings are defined below:

$$CKMR_{target} = \left(\frac{T2-T1}{y2-y1}\right) \cdot (y - y1) + T1 \quad \dots\dots\dots y1 \leq y \leq y2$$

$$CKMR_{target} = T2 \quad \dots\dots\dots y2 < y$$

$$T1=0.5, T2=2.0, y1=2021, y2=2035.$$

It was found that when a single $CKMR_{target}$ value was chosen, the TRO started to decrease in the later projection years after satisfying the TRO tuning requirement for 2035. The value of $CKMR_{target}$ has to be small initially to allow the TAC to increase, but bigger later so that the TAC does not become too large to force TRO to decline after hitting the target.

DMM6

The sixth CMP (DMM6) combines all the CPUE, GT and CKMR data:

$$\begin{aligned}TAC_{y+1}^1 &= TAC_y^1 \times (1 + \beta \cdot (J_y - J_{target})) \\TAC_{y+1}^2 &= TAC_y^2 \times (1 + \gamma \cdot (GTJ_y - GTJ_{target})) \\TAC_{y+1}^3 &= TAC_y^3 \times (1 + \gamma \cdot (CKMR_y - CKMR_{target})) \\TAC_{y+1} &= v \cdot TAC_{y+1}^3 + (1 - v) \cdot [w \cdot TAC_{y+1}^1 + (1 - w) \cdot TAC_{y+1}^2]\end{aligned}$$

The parameters and their values are the same as for DMM4 and DMM5, but an extra parameter v is added. This parameter essentially gives a relative weight to the CKMR compared to the CPUE and gene tagging data. At this stage we set $v=0.5$ for illustrative purposes, leaving optimization of this choice to later. It turned out that this approach happened to achieve the median TRO target for 2035 “automatically” without further tuning being needed.

For all these six CMPs above, TACs are set every third year as a base case (sensitivities to this frequency being every two years have been explored previously and did not impact performance substantially). Furthermore, any

change in the TAC is restricted to a maximum of 3000t (up or down) (sensitivities to this of 2000 and 4000 have also been explored previously, and similarly did not impact performance to any substantial extent). The minimum TAC change limit is 100t. Thus:

$$100 \leq |TAC_{y+1} - TAC_y| \leq 3000, 2000 \text{ or } 4000$$

Results and Discussion

Comparison of DMM2, DMM4, DMM5 and DMM6 performances for the Reference Case.

Figure 1 shows plots of log-linear trends in TRO and of AAV (%) for the projection period. There is no major difference amongst these CMPs in terms of trends in TRO. DMM5 performs slightly better than others in terms of quantile range of the AAV for the “reference case” OM (RC), followed by DMM6.

Figure 2 shows the worm plots for TAC and TRO for these CMPs. All the CMPs show a gradual increase in TAC and TRO, with the trend in TRO stabilizing for the later projection years. For DMM5 the TAC variation is lower initially but gets higher towards the end of the period considered.

DMM4, DMM5 and DMM6 performances across all the Robustness tests.

Figure 3a shows plots of log-linear trends in TRO and of AAV (%) for the projection years for DMM4 for all the robustness tests that were available. These results are based on 2000 replicates. Figure 3b shows the corresponding results for DMM5, and Figure 3c those for DMM6. These were based on 200 replicates only, since the simulations involving the CKMR data require a minimization process which needs much longer computation times. However, the results would not be expected to change qualitatively when increasing from 200 to 2000 replicates. Regardless of the CMP concerned, the OMs that stand out as resulting in performances different from those for the RC are “reclow5 (H: High priority)”, “h55sqrt (M: Medium priority)” and “reclow10 (L: Low priority)”. These show much smaller log-linear trends in TRO compared to the RC. “Cpuew0 (L)” is similar as regards performance differences, in that it shows a very large PI on the trends in TRO. Based on Figures 3a-3c, the following scenarios (“reclow5”, “upq”, “as2016”, “omega75”, “h55sqrt” and “cpuew0”) were compared further amongst the CMPs. The OM “reclow10” was not considered plausible by the OMMP meeting, and hence was not considered for further analyses.

DMM4, DMM5 and DMM6 performances for the selected Robustness tests.

Figure 4 shows plots of log-linear trends in TRO and of AAV (%) for the projection period for the RC and high priority robustness tests (“upq”, “as2016”, “omeg75”), as well as for those that were identified as differing appreciably in performance compared to the RC (“h55sqrt (M)”, and “cpuew0 (L)”) for DMM4, DMM5 and DMM6. There are no major differences among the CMPs with respect to the trends in TRO. The PIs for AAV are narrowest for DMM5; however, performance is better for DMM6 for the cases of “reclow5” and “cpuew0” with a lower median and PI for AAV. There are fewer instances of TRO reducing after 2035 for DMM6 compared to DMM5.

Conclusions

For the RC OM alone, the DMM5 CMP based on the CKMR data only seems to perform the best overall, but when the robustness tests making the greatest impacts are also taken into account, the DMM6 CMP based on all three sets of data available for input seems marginally better.

Further analyses

Some further exploration of the best relative weighting to give to the contributions from the three types of data in DMM6 might produce marginally improved performance.

Furthermore, the 95 % probability envelopes shown in Figure 2 hide the fact that ranging from about 0.5 to 1% of the trajectories for both the TAC and TRO across DMM4 to DMM5 (with DMM6 intermediate) start dropping rapidly towards zero soon after 2035, which is an issue that needs to be addressed.

However, plans for further work on both these matters might better first await feedback from discussions to be held at the September ESC meeting. For example, should specific metarules be developed to eliminate the behavior noted in the paragraph above; or rather, since this starts to occur only almost 20 years into the future, with a number of updates in assessments and MP revisions due before that time, is it a matter better left for now to be addressed after some of these updates and revisions have taken place?

Acknowledgments

We thank Richard Hillary for use of his code for developing a TRO index from the CKMR data, and Darcy Webber for assistance with the trials code.

References

- Butterworth, D.S., Miyagawa, M. and Jacobs, M.R.A. 2018. Initial exploratory investigations of some simple candidate management procedures for southern Bluefin tuna. Paper presented to the CCSBT OMMP meeting, Seattle, 18-22 June 2018. CCSBT-OMMP/1806/12: 18pp.
- Hillary, R., Preece, A. and Davies, C. 2018. Initial MP structure and performance. Paper presented to the CCSBT OMMP meeting, Seattle, 18-22 June 2018. CCSBT-OMMP/1806/05: 14pp.

Table 1. Some performance statistics for DMM4, 5 and 6 for the “RC (base16)” and selected six robustness tests (“as2016”, “reclow5”, “upq”, “cpuew0”, “h55sqrt” and ”omega75”). Median values are shown for the distributions for each statistic. Recall that each CMP is tuned to achieve a median TRO in 2035 which is 30% of its pristine value for the RC (base 16) OM.

Tuning	CMP	Run	Mean TAC ₍₂₀₂₁₋₂₀₃₅₎	Mean TAC ₍₂₀₃₆₋₂₀₅₀₎	AAV (%)	TRO ₂₀₃₅ /TRO ₀	TRO ₂₀₅₀ /TRO ₀	TRO ₂₀₃₅ /TRO ₂₀₁₈	TRO ₂₀₅₀ /TRO ₂₀₁₈	Min. TRO ₂₀₁₉₋₂₀₃₅ /TRO ₀	70% > 0.2TRO ₀
30	DMM4_3000	base16	20417	27423	5.16	0.3	0.3	2.02	2	0.16	2022
		as2016	19760	25414	4.03	0.24	0.27	1.73	1.93	0.14	2025
		reclow5	18770	20544	1.64	0.24	0.33	1.59	2.2	0.16	2022
		upq	20497	27528	5.32	0.25	0.24	1.95	1.85	0.14	2024
		cpuew0	18744	20966	1.8	0.16	0.18	1.82	2.06	0.09	2032
		h55sqrt	19849	24784	3.99	0.22	0.21	1.57	1.5	0.15	2022
		omega75	19967	25867	4.37	0.3	0.32	2.12	2.31	0.15	2022
	DMM5_3000	base16	20427	25610	4.15	0.3	0.32	2.01	2.2	0.16	2022
		as2016	20115	21630	3.12	0.23	0.3	1.69	2.16	0.14	2025
		reclow5	20382	21795	3.91	0.22	0.27	1.48	1.8	0.15	2022
		upq	20210	24043	3.53	0.25	0.29	1.96	2.22	0.14	2024
		cpuew0	19520	18985	2.48	0.15	0.17	1.71	1.96	0.09	2032
		h55sqrt	20248	21261	3.42	0.22	0.24	1.54	1.64	0.15	2022
		omega75	20515	27127	4.58	0.29	0.31	2.07	2.19	0.15	2022
	DMM6_3000	base16	20444	26864	4.76	0.3	0.31	2.01	2.06	0.16	2022
		as2016	19983	23778	3.57	0.24	0.28	1.72	2.01	0.14	2025
		reclow5	19569	21364	2.61	0.23	0.29	1.53	1.96	0.15	2022
		upq	20389	25955	4.49	0.26	0.25	1.96	1.98	0.14	2024
		cpuew0	19159	20217	1.97	0.15	0.17	1.75	1.98	0.09	2032
		h55sqrt	20088	23244	3.78	0.22	0.22	1.55	1.56	0.15	2022
		omega75	20284	26949	4.57	0.3	0.3	2.1	2.19	0.15	2022

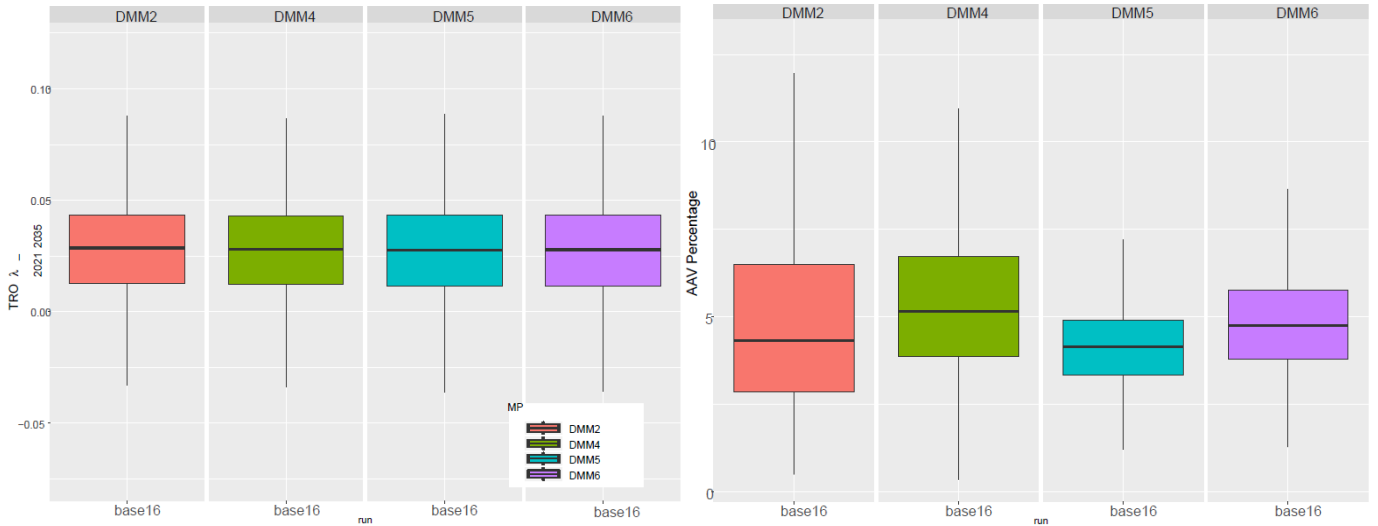


Figure 1. Plots of Log-linear trends in TRO from 2021 to 2035 (left) and AAV (%) from 2021 to 2035 (right) for DMM2, 4, 5 and 6 for the “reference case” (RC) scenario.

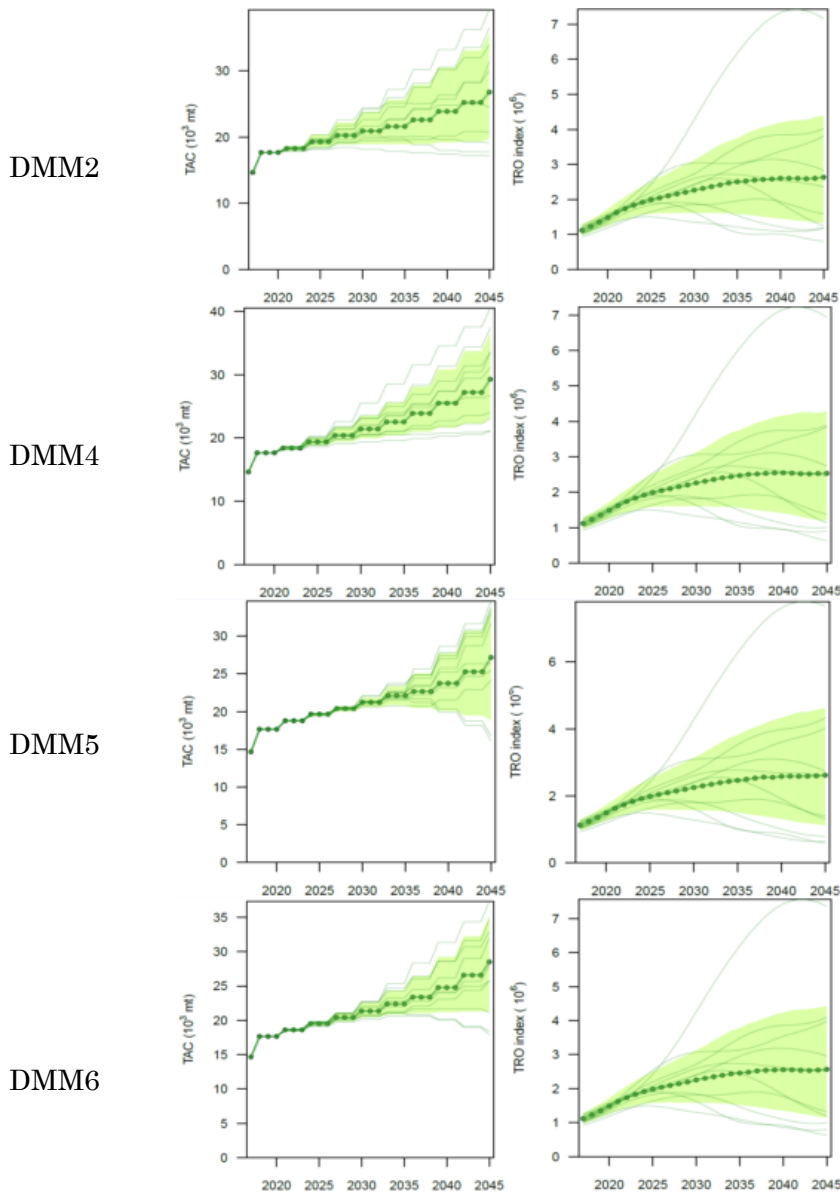


Figure 2. Worm plots for TAC and TRO for DMM2,4, 5 and 6 for the RC, when tuned to 30% of TRO_0 in the year 2035. The green shadings represent 95% probability envelopes.

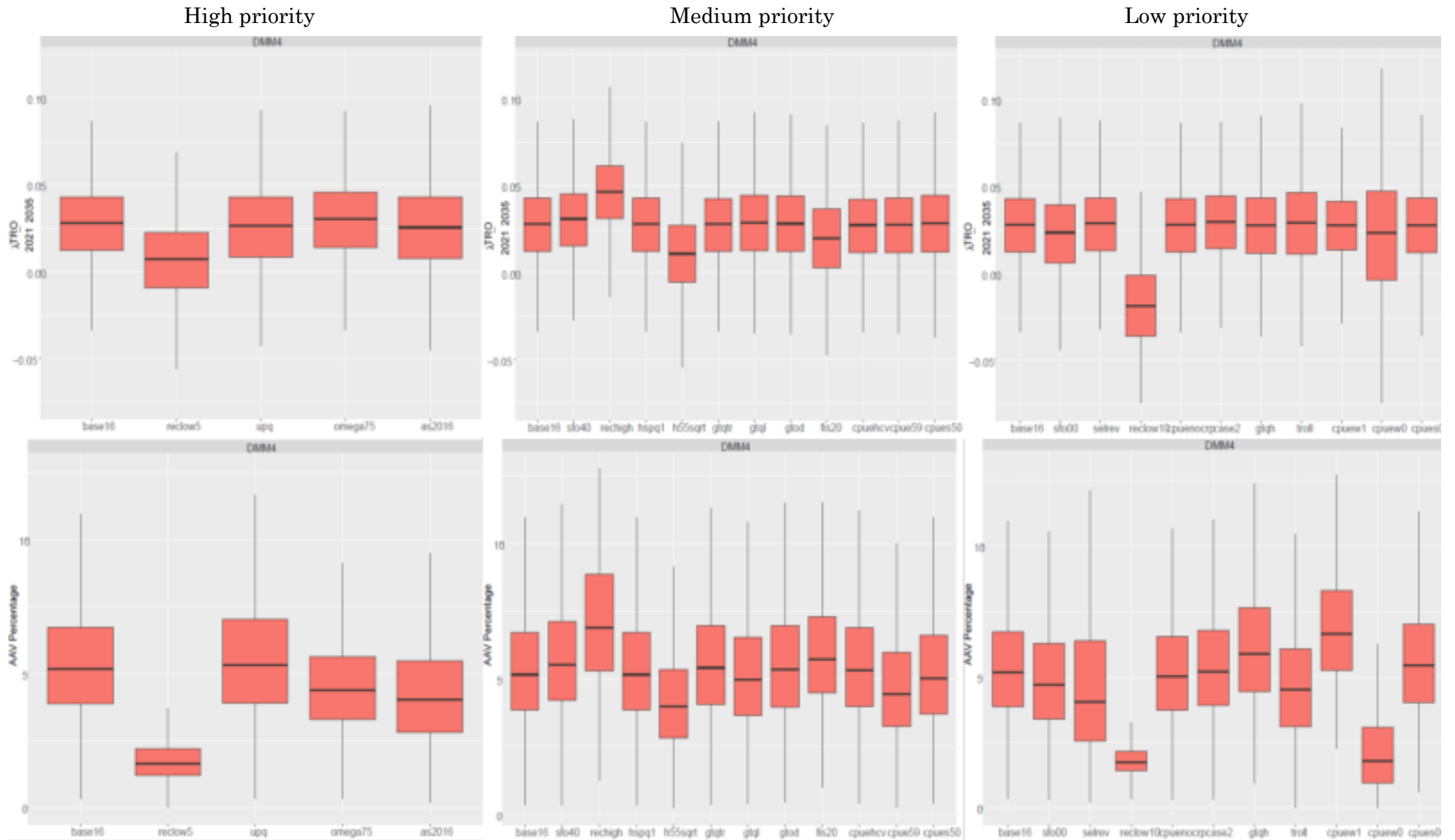


Figure 3a. Plots of Log-linear trends in TRO from 2021 to 2035 (top) and AAV (%) from 2021 to 2035 (bottom) for **DMM4** for the various robustness tests scenarios categorized into High, Medium and Low priorities (based on 2000 runs). The lower and upper hinges correspond to the first and third quartiles (the 25th and 75th percentiles). The upper whisker extends from the hinge to the largest value no further than $1.5 * IQR$ from the hinge (where IQR is the inter-quartile range, or distance between the first and third quartiles). The lower whisker extends from the hinge to the smallest value at most $1.5 * IQR$ of the hinge.

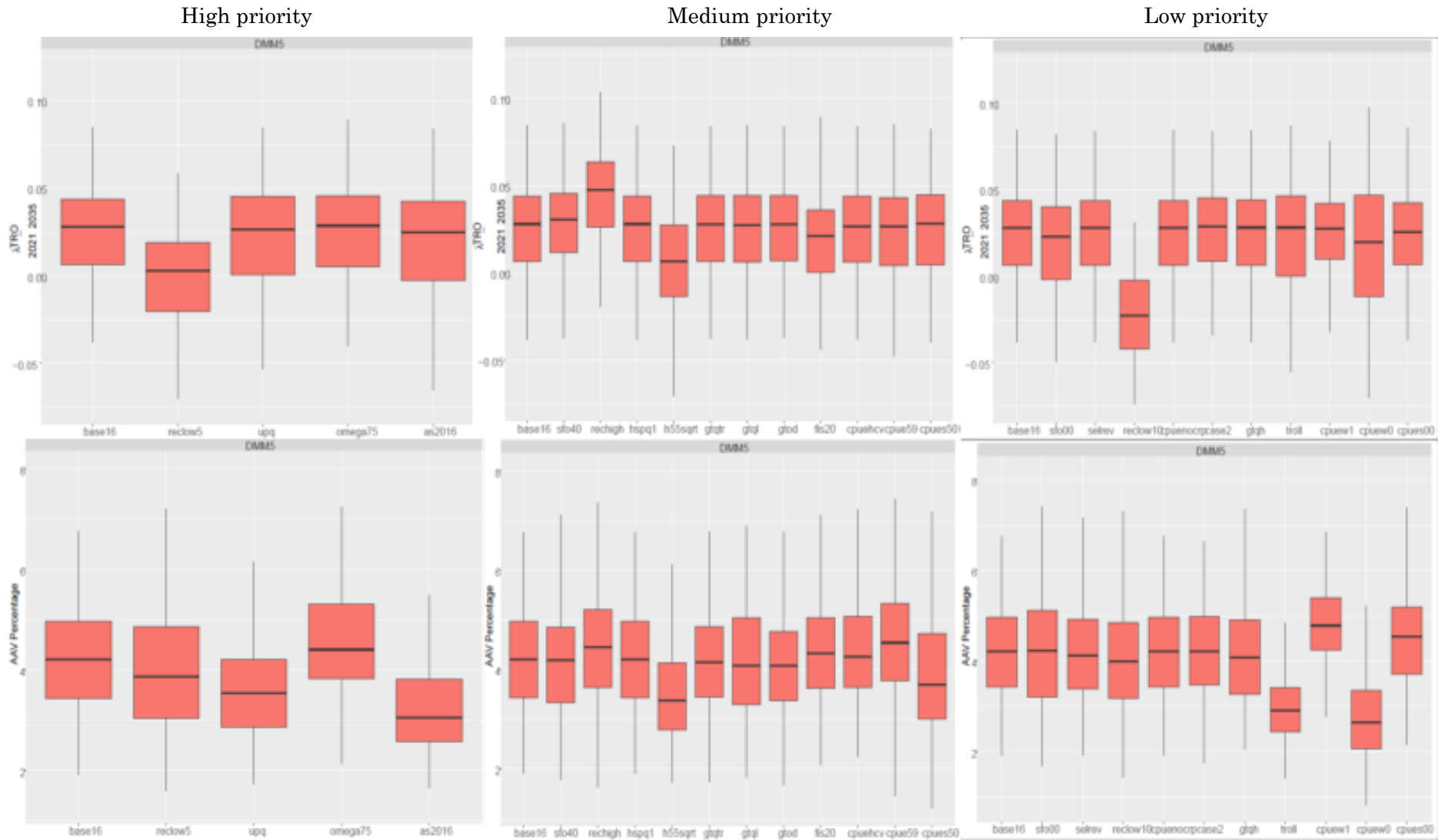


Figure 3b. Plots of Log-linear trends in TRO from 2021 to 2035 (top) and AAV (%) from 2021 to 2035 (bottom) for **DMM5** for the various robustness tests scenarios categorized into High, Medium and Low priorities (based on 200 runs). The lower and upper hinges correspond to the first and third quartiles (the 25th and 75th percentiles). The upper whisker extends from the hinge to the largest value no further than $1.5 * IQR$ from the hinge (where IQR is the inter-quartile range, or distance between the first and third quartiles). The lower whisker extends from the hinge to the smallest value at most $1.5 * IQR$ of the hinge.

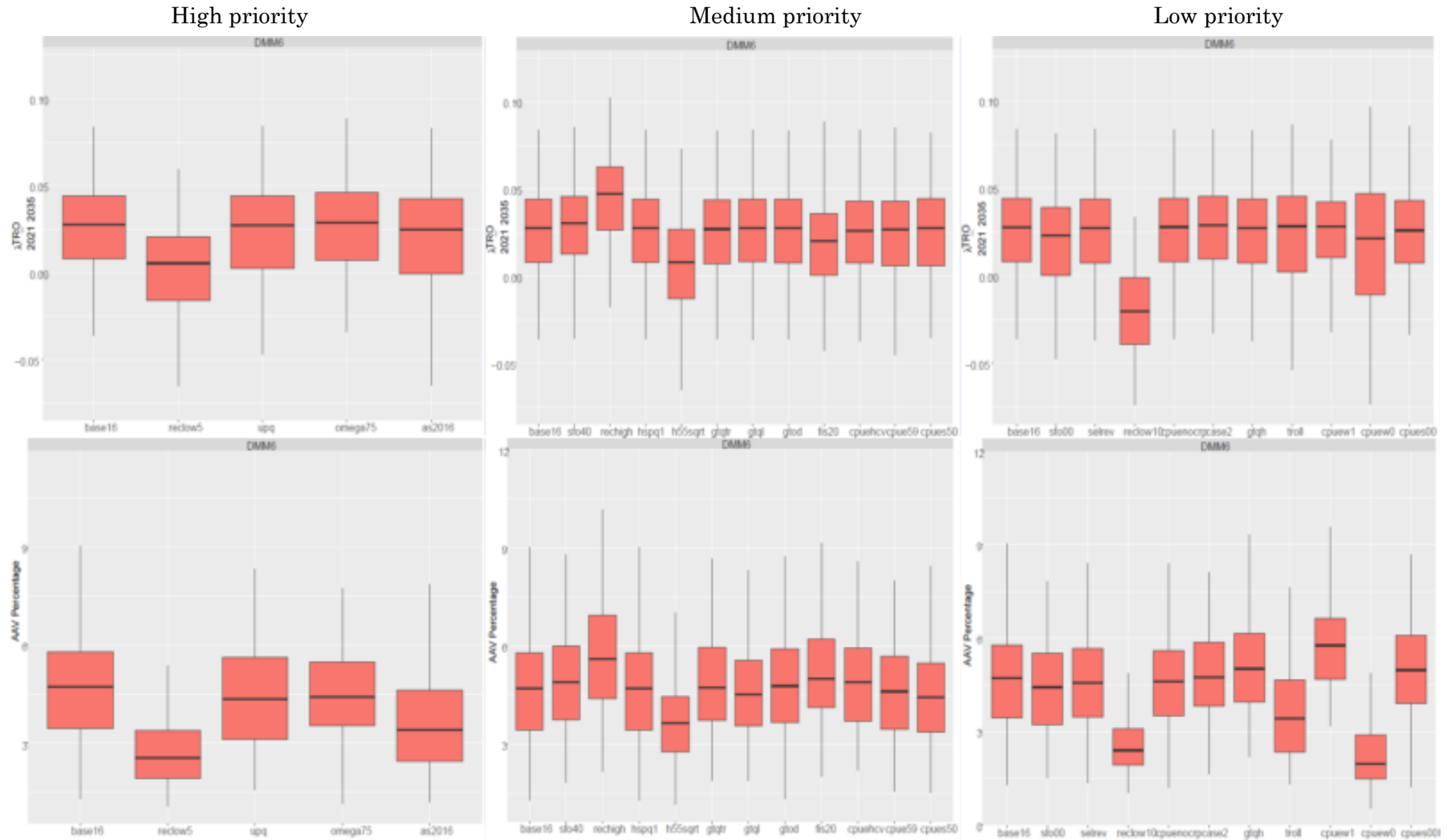


Figure 3c. Plots of Log-linear trends in TRO from 2021 to 2035 (top) and AAV (%) from 2021 to 2035 (bottom) for **DMM6** for the various robustness tests scenarios categorized into High, Medium and Low priorities (based on 200 runs). The lower and upper hinges correspond to the first and third quartiles (the 25th and 75th percentiles). The upper whisker extends from the hinge to the largest value no further than $1.5 \cdot \text{IQR}$ from the hinge (where IQR is the inter-quartile range, or distance between the first and third quartiles). The lower whisker extends from the hinge to the smallest value at most $1.5 \cdot \text{IQR}$ of the hinge.

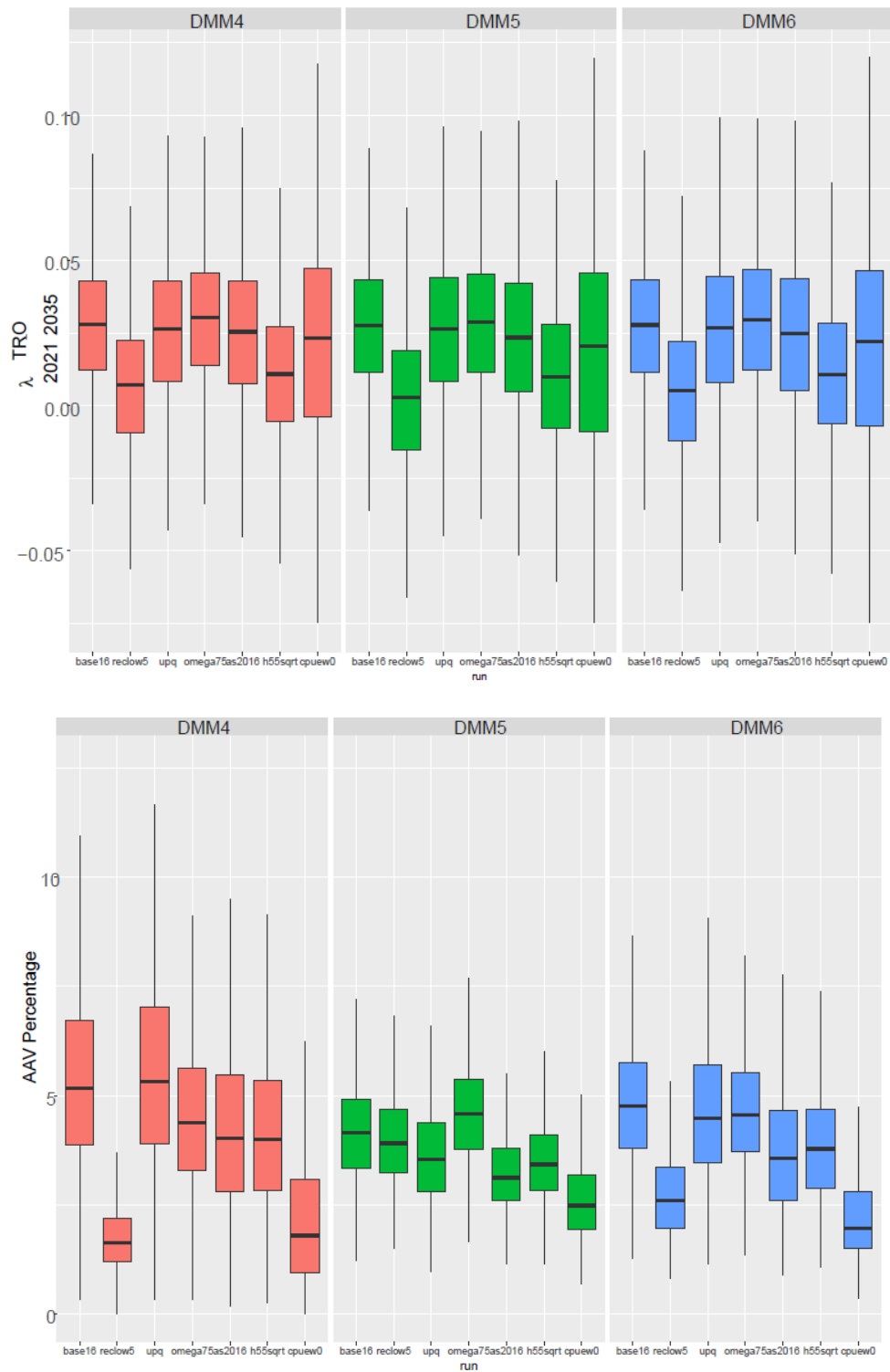


Figure 4. Plots of Log-linear trends in TRO from 2021 to 2035 (top) and AAV(%) from 2021 to 2035 (bottom) for DMM4, DMM5 and DMM6 for the “reference case” selected robustness test scenarios: “upq (H)”, “as2016(H)”, “omega75(H)”, “h55sqrt(M)”, and “cpuew0(L)”. All results are based on 2000 replicates. The lower and upper hinges correspond to the first and third quartiles (the 25th and 75th percentiles). The upper whisker extends from the hinge to the largest value no further than $1.5 * IQR$ from the hinge (where IQR is the inter-quartile range, or distance between the first and third quartiles). The lower whisker extends from the hinge to the smallest value at most $1.5 * IQR$ of the hinge.